Quasi-uncoupled rotational diffusion of phospholipid headgroups from the main molecular frame

Hanne S. Antila,[1] Anika Wurl,[2] O. H. Samuli Ollila,[3] Markus S. Miettinen,[1] and Tiago M. Ferreira[2,*]

[1]*Department of Theory and Bio-Systems, Max Planck Institute of Colloids and Interfaces, 14424 Potsdam, Germany*
[2]*Institute for Physics, Martin-Luther University Halle-Wittenberg*
[3]*Institute of Biotechnology, University of Helsinki, 00014 Helsinki, Finland*

(Dated: September 16, 2020)

Understanding the dynamics of phospholipid headgroups in model and biological membranes is of extreme importance for an accurate description of the dipolar interactions occuring at membrane interfaces. One fundamental question is to which extent these dynamics are coupled to an overall molecular frame i.e. if the dipole headgroup orientation distribution and time-scales involved depend on the structure and dynamics of the glycerol backbone and hydrophobic regions or if this motion is independent from the main molecular frame. Here we use solid-state nuclear magnetic resonance (NMR) spectroscopy and molecular dynamics (MD) simulations to show that the orientation and effective correlation times of choline headgroups remain completely unchanged with 50% mol cholesterol incorporation in a phosphatidylcholine (PC) membrane in contrast to the significant slowdown of the remaining phospholipid segments. Notably, our results indicate that choline headgroups interact as quasi-freely rotating dipoles at the interface irrespectively of the structural and dynamical molecular behavior in the glycerol backbone and hydrophobic regions to the full extent of headgroup rotational dynamics.

Cells rely on rather complex processes to synthetize and mantain specific locations of a myriad of different phospholipids in cellular membranes for compartmentalization, signaling and transport functions. Membrane composition is a result of molecular evolution and a variety of phospholipid membrane compositions are found in nature depending on cell types, organelles and species [1]. Among such diversity, one common feature to most if not all biological membranes is the ubiquitous dominant presence of di-acyl phosphatidycholine (PC) and/or di-acyl phosphatidylethanolamine (PE) with nearly identical chemical structures corresponding to a glycerol backbone linked to two acyl chains and a negatively charged phosphate group bearing a positively charged choline head group, $–CH_2CH_2N(CH_3)_3^+$, or ethanolamine head group, $–CH_2CH_2NH_3^+$, respectively. Accordingly, the surface of cell membranes is highly populated of phospholipid headgroup dipoles which contribute in a non-trivial way to the membrane electrostatic potential.

The P^-–N^+ dipole orientation and dynamics has been thoroughly investigated for a number of PC and PE bilayer systems [2–19] . Among the previous investigations, one fundamental question arises. To which degree is the orientational behaviour of the surface dipoles related to the molecular body at which they are attached? Two limiting cases may be considered, (a) that the dipoles are nearly or fully uncoupled from the rigid-body acting as quasi-Keesom dipoles which are positionally fixed but quasi-free to reorient according to local electrostatic interactions or (b) that the orientation and dynamic time-scales for headgroup orientation are largely affected by the structure and dynamics of the phospholipid molecules as a whole and therefore dependent on e.g. time-scales of motion of the glycerol backbone and hydrophobic acyl chains.

From a purely structural standpoint, an independence of the orientation of the headgroup from the hydrophobic region stands out from analysing the previously measured NMR C–H bond order parameters, $S_{\mathrm{CH}} = \langle 1/2(3\cos^2\theta - 1)\rangle$, where θ denotes the angle between the C–H bond and the bilayer normal and the angular brackets denote a time-average. NMR order parameter values are the most accurate observables with atomistic resolution measured from phospholipid bilayers up until present. A close look on the large set of previously reported S_{CH} values for the α and β positions of the choline headgroup, shows that for all the distinct PC bilayers at full hydration measured in the liquid crystalline phase (L_α), the S^{β}_{CH} values lie on a range between -0.05 and -0.02, while S^{α}_{CH} is equal to +0.05±0.005. Table I shows some of the previously measured systems. The α order parameter falls within such extremely narrow range not only between different systems but remarkably also regardless of temperature. A structural analysis based on the α and β order parameters is ill-defined since a range of semirigid and mobile empirical models can simultaneously fit the set of α and β order parameters [8], however to highlight the stability of the choline orientation/conformation over the different systems it is relevant to note that the wider range of the β order parameters may be induced by a change in the α-β torsion angle of only 2-3° [7] in a semi-rigid fully empirical model [5].

Irrespectively of the molecular model considered, the constant value of the α C–H bond order parameter indicates that the structure of the headgroup is not affected by the molecular structure in the acyl chain region which changes considerably among the different systems and with temperature. It is known though that the headgroup orientation is highly sensitive to a decrease of hydration [21], to the inclusion of charges [14] and molecular dipoles [23], to the presence of salt ions [24] and to the hydrostatic pressure [15], with S^{α}_{CH} ranging from -0.02 to +0.1. This is exemplified also in table I for DMPC at a hydration of approximately 10 water molecules per lipid with an increase of $|S^{\alpha}_{\mathrm{CH}}|$ to 0.07±0.005 showing again an independent orientation on temperature.

From the order parameters alone one cannot draw however any conclusion on how the time-scales of motion in the different systems are affected, since the order parameters relate only to the distribution of C–H bond orientations but not to how

System	T / °C	Phase	S^{α}_{CH}	$-S^{\beta}_{\mathrm{CH}}$	ref.
DMPC	25-35	L_{α}	0.05	0.05-0.04	[20]
	20	L_{β}	0.05	0.06	
DOPC	30	L_{α}	0.05	0.03	[21]
POPC	23	L_{α}	0.05	0.04	[22]
DPPC	45-90	L_{α}	0.05	0.05-0.02	[4]
DPPC/chol. (1:1)	10-70	L_{α}	0.05	0.03-0.02	[7]
POPC/chol. (1:1)	30	L_{α}	0.05	0.04	here
DMPC	27	L_{α}	0.07	0.05	here
n_w/n_l=10	57	L_{α}	0.07	0.03	

TABLE I: Previously published α and β C–H bond order parameters from ^{2}H NMR spectroscopy for a number of phosphatidylcholine lamellar systems together with values reported here using ^{1}H-^{13}C dipolar recoupling on DMPC and POPC/cholesterol (1:1). All systems were near to full hydration except for the DMPC samples at a water to lipid molar ratio approximatelly equal to 10. The $|S_{\mathrm{CH}}|$ accurate values lie within $\pm$0.005 of the values presented. The order parameter for DPPC/chol (1:1) is the average between the inequivalent C–H bond order parameters reported.

fast such configuration space is spanned. To assess the effect on the time-scales of motion, NMR relaxation experiments can be used to measure relaxation rates, e.g. the spin-lattice relaxation R_1 and the spin-lattice relaxation in the rotating frame $R_{1\rho}$, which depend on spectral density terms, $J(\omega_i)$, where the relevant frequencies ω_i depend on the strength of the magnetic field, experimental setup and nuclei used, and the spectral density, $J(\omega)$, is the Fourier transform of the orientation autocorrelation function of a given molecular-fixed axis [18, 25–28]. Klauda et al. [18] compared the experimental ^{31}P R_1 dispersion of DPPC vesicles from 0.022 to 21.1 T to all-atom molecular dynamics simulations using the CHARMM C27r force-field and found good agreement between simulation and experiments. The motion predicted by the simulation was then analysed with an often used relaxation model for fitting relaxation dispersion data, containing wobble and axial rotation of the overall lipid body and fast internal motion. Based on this analysis, Klauda and coworkers suggested a partial uncoupled motion of the headgroup from the overall lipid body since though the model fitted extremely well the acyl chain and glycerol backbone motions together it did not extend successfully to the choline segments. The uncoupled motion in the CHARMM C27r model was suggested to be due to a relatively free rotation around the P–O(-g$_3$) bond that connects the phosphate group to the glycerol backbone based on the potential mean force profile for this torsion angle [18]. A free rotation around the g_3–g_2 bond as also been previously suggested by Seelig et al.[4] and indeed the dihedral torsion potential for this bond in CHARMM C36 (an update of CHARMM C27r for lipids) assumes free rotation.

To which extent the motion is uncoupled can be investigated by observing how changes in the main molecular frame motional time-scales affect the headgroup dynamics. Roberts and coworkers have later shown experimentally that the phosphorus dynamic time-scales are largely affected by the incorporation of cholesterol presumably due to a slower wobbling motion [29]. A free rotation around the P–O(-g$_3$) bond proposed by Klauda et al. [18] (or around the g_3–g_2 bond) would partially or even fully decouple the headgroup dynamics from the overall rotation of the phospholipid around the bilayer normal, nevertheless a slowdown of the wobble motion timescale could still affect the headgroup motion. However, if the torsion around the P–O(-g$_3$) bond is relatively free, a torsion around the P–O(-α) bond and possibly around other bonds to maintain the choline dipole orientation at some preferential range of angles may also be considered. Such a set of rotations would potentially decouple the dynamics of the headgroup both from the overall rotation around the molecular main frame as well as from the wobble motion and could be responsible for the orientation response of the choline dipole to the local electrostatic interactions. Such a molecular framework would fit in the quasi-Keesom hypothesis.

Here we address the effect of the wobble and rotational slowdown of the main molecular frame on the dipolar headgroup using our previously reported methodology to translate S_{CH}, R_1 and $R_{1\rho}$ values into C–H bond effective correlation times [28]. Figure 1 shows how the ^{13}C R_1 and $R_{1\rho}$, τ_e observables of POPC multilamellar vesicles change with the incorporation of cholesterol. The experiments were done under a static magnetic field inducing a Larmor frequency equal to 500 MHz for ^{1}H and a spin lock field for $R_{1\rho}$ of 50 kHz. The fits used to determine the presented values are given as supplementary information. Note that a value of 50 kHz for the spin lock field ensures that $R_{1\rho}$ is only sensitive to motions within the fast motion regime and that contributions from possible collective motions and from diffusion over vesicles can be neglected [28]. The striking observation is that both the R_1, $R_{1\rho}$ and τ_e values for the α and β segments remain exactly the same within experimental uncertainty in contrast to the glycerol backbone slowdown, here quantified to be approximately two times slower. This result is remarkable since it shows that the headgroup reorientation motion is not only partially uncoupled from the glycerol backbone as previously suggested but that the dipole motion of PC headgroups is fully independent of the overall motion of the main molecular frame and therefore insensitive to changes in the glycerol backbone motional time-scales and the presence of cholesterol in the bilayer. Previously, ^{13}C $R_{1\rho}$ measurements have been reported showing a slight increase of $R_{1\rho}$ for the α and β segments induced by cholesterol incorporation in DMPC bilayers. However, it is hard to judge how statistically significant were those changes since no error bars have been reported [30].

In addition to the experimental demonstration presented, we show that among four widely used MD force fields Slipids, CHARMM C36, MacRog and Berger lipids, only CHARMM C36 and Slipids predicts this result. By comparing the segmental effective correlation times with the experimental ones, nearly perfect quantitative agreement within the experimental and simulation uncertainties is obtained for the Slipids and

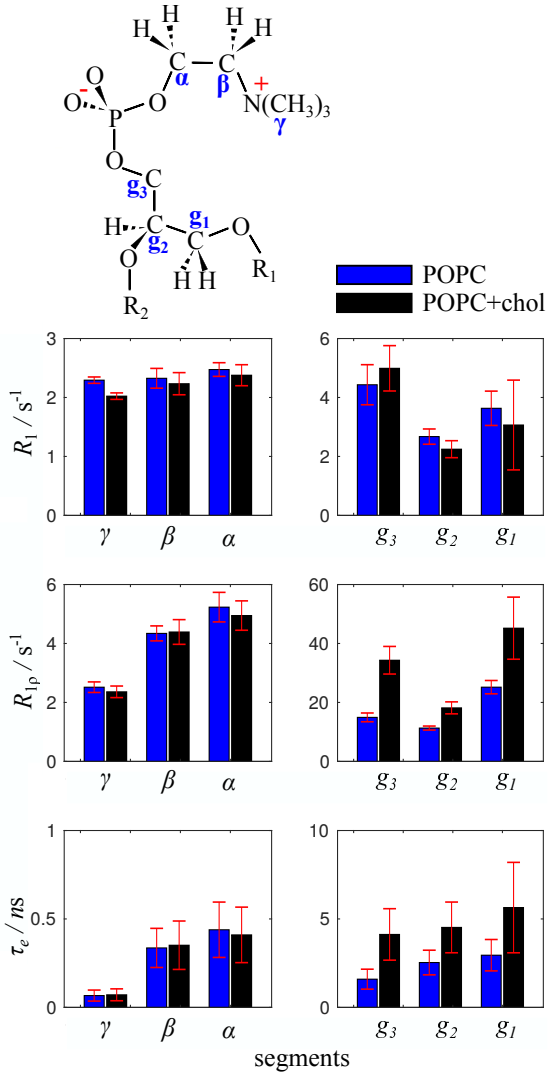

FIG. 1: Effect of cholesterol on the ^{13}C spin-lattice relaxation R_1, spin-lattice relaxation in the rotating frame $R_{1\rho}$, and on the effective correlation times τ_e of the different segments in the headgroup and glycerol backbone of POPC.

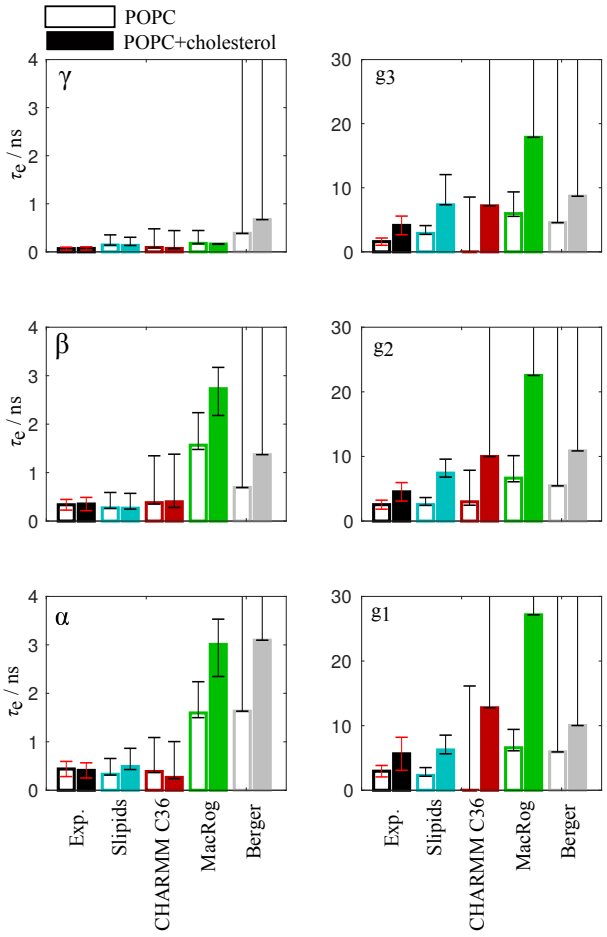

FIG. 2: Comparison of the effective correlation time profiles predicted by the Slipids, CHARMM C36, MacRog and Berger force-fields for the headgroup and glycerol backbone with the experimental values measured.

CHARMM-C36 force fields. The MacRog and Berger force fields predict a slowdown of the headgroup with incorporation of cholesterol and fail to provide good quantitative estimates of τ_e for both the systems with and without cholesterol, indicating that these force-fields include an erroneous coupling of the headgroup with the main molecular body. A comparison of simulated and experimental R_1 and $S_{\rm CH}$ values is also given as SI. We are now planning a number of experiments and simulations on PC and PE systems to investigate such behaviour with more detail focusing on detailed conformational changes.

The experimental results (and the more realistic simulations) support the quasi-Keesom hypothesis considered above where the dipole orientation fully depends on the local electrostatic interactions while fully uncoupled from the rest of the lipid molecular body. As noted above, it is well known that the headgroup conformation/orientation can react strongly to the inclusion of charges [20] or dipoles [23] in the membrane with a consequent variation of the α order parameter as well as to the level of hydration [21, 22], salt concentration [24], and hydrostatic pressure [15]. It is yet to be investigated how such changes on the orientation distribution affect the headgroup dynamic time-scales.

The molecular description here presented has rather strong implications for membrane biophysics and should motivate a number of additional experiments and simulations. It implies that the dipolar surface of bilayers with lipids having the same headgroup but distinct acyl chains will have additionally to the same headgroup orientation the same dynamic time-scales, as well in mixtures of these phospholipids with cholesterol. The dynamics of dipolar headgroups in bilayers consisting of mixtures of phospholipids with different headgroups may also be independent of the acyl chains involved and dominated by the dipole-dipole interactions between the distinct dipoles. This needs however to be tested since e.g. PE headgroups have

a different orientation than PC headgroups at full hydration and may therefore have a different behaviour. The results presented here do not support the assumption in the *umbrella model* that headgroups reorient when cholesterol is present in the bilayer in order to shield the cholesterol interfacial cross section from water molecules[31].

In summary, our results suggest that for describing the dipolar interactions at the surface of membranes, the hydrophobic structure may be neglected to a good approximation and that the relevant headgroup physics lie on the electrostatic interactions, which would be remarkably useful considering the complex molecular arrangement in the hydrophobic region of biological membranes.

TMF greatly acknowledges Kay Saalwächter and Alexey Krushelnitsky for invaluable support and discussions.

* tiago.ferreira@physik.uni-halle.de

[1] D. Marsh, *Handbook of Lipid Bilayers* (CRC press, New York, 2013).

[2] R. Griffin, J. Am. Chem. Soc. **98**, 851 (1976), URL https://doi.org/10.1021/ja00419a044.

[3] S. Kohler and M. Klein, Biochemistry **16**, 519 (1977), URL http://dx.doi.org/10.1021/bi00622a028.

[4] H. Gally, W. Niederberger, and J. Seelig, Biochemistry **14**, 3647 (1975), URL https://doi.org/10.1021/bi00687a021.

[5] J. Seelig, H.-U. Gally, and R. Wohlgemuth, BBA - Biomembranes **467**, 109 (1977), URL http://www.sciencedirect.com/science/article/pii/0005273677900128.

[6] R. Griffin, L. Powers, and P. Pershan, Biochemistry **17**, 2718 (1978), URL https://doi.org/10.1021/bi00607a004.

[7] M. Brown and J. Seelig, Biochemistry **17**, 381 (1978), URL https://doi.org/10.1021/bi00595a029.

[8] R. Skarjune and E. Oldfield, Biochemistry **18**, 5903 (1979), URL https://doi.org/10.1021/bi00593a022.

[9] S. Rajan, S. Kang, H. Gutowsky, and O. E, J Biol Chem. **256**, 1160 (1981), URL http://www.jbc.org/content/256/3/1160.short.

[10] D. Siminovitch, M. Rance, and K. Jeffrey, FEBS Letters **112**, 79 (1980), ISSN 0014-5793, URL http://www.sciencedirect.com/science/article/pii/0014579380801323.

[11] T. Rothgeb and E. Oldfield, J Biol Chem. **256**, 6004 (1981), URL http://www.jbc.org/content/256/12/6004.short.

[12] R. Ghosh, Biochemistry **27**, 7750 (1988), URL https://doi.org/10.1021/bi00420a025.

[13] M. Milburn and K. Jeffrey, Biophys J. **56**, 543 (1989), URL https://doi.org/10.1016/S0006-3495(89)82701-8.

[14] P. Macdonald, J. Leisen, and F. Marassi, Biochemistry **30**, 3558 (1991), URL http://dx.doi.org/10.1021/bi00228a029.

[15] B. Bonev and M. Morrow, Biophys J. **69**, 518 (1995), URL https://doi.org/10.1016/S0006-3495(95)79925-8.

[16] M. Roberts and A. Redfield, **101**, 17066 (2004).

[17] M. U. Roberts MF, Redfield AG, Biophys J. **97**, 132 (2009), URL https://doi.org/10.1016/j.bpj.2009.03.057.

[18] J. Klauda, M. Roberts, A. Redfield, B. Brooks, and R. Pastor, Biophys J. **94**, 3074 (2008), URL http://www.sciencedirect.com/science/article/pii/S0

[19] J. Doux, B. Hall, and J. Killian, Biophys J. **103**, 1245 (2012), URL http://dx.doi.org/10.1016/j.bpj.2012.08.031.

[20] P. Macdonald, J. Leisen, and F. Marassi, Biochemistry **30**, 3558 (1991), URL https://doi.org/10.1021/bi00228a029.

[21] A. Ulrich and A. Watts, Biophys. J. **66**, 1441 (1994), URL https://doi.org/10.1016/S0006-3495(94)80934-8.

[22] B. Bechinger and J. Seelig, Chemistry and Physics of Lipids **58**, 1 (1991), URL http://www.sciencedirect.com/science/article/pii/00

[23] B. Bechinger and J. Seelig, Biochemistry **30**, 3923 (1991), URL https://doi.org/10.1021/bi00230a017.

[24] C. Altenbach and J. Seelig, Biochemistry **23**, 3913 (1984), URL https://doi.org/10.1021/bi00312a019.

[25] M. Brown, J. Seelig, and U. Häberlen, J. Chem. Phys. **70**, 5045 (1979), URL https://doi.org/10.1063/1.437346.

[26] M. Brown, A. Ribeiro, and G. Williams, Proc. Natl. Acad. Sci. USA **80**, 4325 (1983), URL https://doi.org/10.1073/pnas.80.14.4325.

[27] C. Morrison and M. Bloom, J. Chem. Phys. **101**, 749 (1994), URL https://doi.org/10.1063/1.468491.

[28] T. Ferreira, O. Samuli, R. Pigliapochi, A. Dabkowska, and D. Topgaard, J. Chem. Phys. **142**, 044905 (2015), URL https://doi.org/10.1063/1.4906274.

[29] V. Sivanandam, J. Cai, A. Redfield, and M. Roberts, J. Am. Chem. Soc. **131**, 3420 (2009), URL https://doi.org/10.1021/ja808431h.

[30] C. Le Guernevé and M. Auger, Biophys J. **68**, 1952 (1995), URL https://doi.org/10.1016/S0006-3495(95)80372-3.

[31] J. Dai, M. Alwarawrah, and J. Huang, J. Phys. Chem. B **114**, 840 (2010), URL https://doi.org/10.1021/jp909061h.

[32] L. Löser, K. Saalwächter, and T. Ferreira, Phys. Chem. Chem. Phys. **20**, 9751 (2018), URL http://dx.doi.org/10.1039/C8CP01012A.

[33] T. Ferreira, F. Coreta-Gomes, O. Ollila, M. Moreno, W. L. Vaz, and D. Topgaard, Phys. Chem. Chem. Phys. **15**, 1976 (2013), URL http://dx.doi.org/10.1039/C2CP42738A.

SUPPLEMENTARY INFORMATION

METHODS

Sample Preparation

The phospholipids 1-palmitoyl,2-oleoyl-sn-glycero-3-phosphocholine (POPC) and 1,2-dimyristoyl-sn-glycero-3-phosphocholine (DMPC), cholesterol and chlorophorm were purchased from Sigma-Aldrich. The samples were prepared by mixing the lipids with chlorophorm and rapidly evaporating the organic solvent under a nitrogen gas flow and subsequently drying the lipid film under vacuum overnight. The film was then hydrated in a 0.5 ml EPPENDORF tube by adding 40 %wt of water and manually mixing with a thin metal rod multiple times alternated by sample centrifugation until a homogeneous mixture was visually attained. The resulting mixture was then centrifuged into a KEL-F Bruker insert with a sample volume of approximatelly 25 μl specifically designed for solid-state NMR 4mm rotors.

To obtain the low hydration sample, a glass tube containing a DMPC film of 20 mg was left for 1 day in a desiccator (volume of approx. 1l) together with a glass tube containing 2 ml of water under reduced pressure. The water content was then determined from integrating the water and γ peaks in the ^{1}H spectra.

NMR Experiments

The R_1 and $R_{1\rho}$ experiments were performed on a a Bruker Avance II-500 NMR spectrometer operating at a ^{13}C Larmor frequency of 125.78 MHz equipped with a a E-free CP-MAS 4 mm (13C/31P/1H). The R-PDLF measurements were performed on a Bruker Avance III 400 spectrometer operating at a ^{1}H Larmor frequency of 400.03 MHz equiped with a standard 4 mm CP-MAS HXY probe. All experiments were performed under magic-angle spinning conditions at a rate of 5 kHz. The processing of all NMR data was done with MATLAB 2018b. The R-PDLF, R_1 and $R_{1\rho}$ experiments were performed as previously described in references [28, 32].

The parameters used were the following. *R-PDLF experiments*: a total of 32 points in the indirect dimension with increments equal to two R18 blocks; SPINAL64 was used for proton decoupling during ^{13}C acquisition, with a nutation frequency of approximately 50 kHz, a total acquisition time of 0.07 s and a spectral width of 200 ppm; the rINEPT pulses were set at a nutation frequency of 78.12 kHz. R_1 and $R_{1\rho}$ *experiments*: RF $\pi/2$ and π pulses were set to a nutation frequency of 63.45 kHz. TPPM was used for proton decoupling during ^{13}C acquisition, with a nutation frequency of approximatelly 50 kHz, a total acquisition time of 0.1 s, recycle delay of 10 s and a spectral width of 140 ppm. The spin-lock frequency for $R_{1\rho}$ was 50 kHz.

For determining R_1 and $R_{1\rho}$ for a given carbon segment, we determined the decay over the indirect dimension by fitting gaussian lineshapes in the direct dimension and using the analytic areas of the fitted functions. The decay was then fitted with a single exponential decay and the error bounds for both the R_1 and $R_{1\rho}$ values presented are the 95 % confidence bounds from these fits. For estimating τ_e we used [28],

$$\tau_e = \frac{5R_{1\rho} - 3.82R_1}{4\pi^2 d_{\mathrm{CH}}^2 N(1 - S_{\mathrm{CH}}^2)} \tag{1}$$

where the rigid coupling constant d_{CH} value used was 20 kHz and the S_{CH} values used were taken from reference [33]. The error, ϵ, for the effective correlation times calculated then becomes,

$$\epsilon(\tau_e) = \frac{5\epsilon(R_{1\rho}) + 3.82\epsilon(R_1)}{4\pi^2 d_{\mathrm{CH}}^2 N(1 - S_{\mathrm{CH}}^2)} \tag{2}$$

For determining the coupling constants with R-PDLF spectroscopy presented in table I, a fit of the time domain data was done by using time domain profiles from numerical simulations of the R-PDLF pulse sequence that take into account the B_1 inhomogeneity of the used CP-MAS probe. This procedure gives an accuracy which is about ten times higher than using frequency domain data and will be described elsewhere.

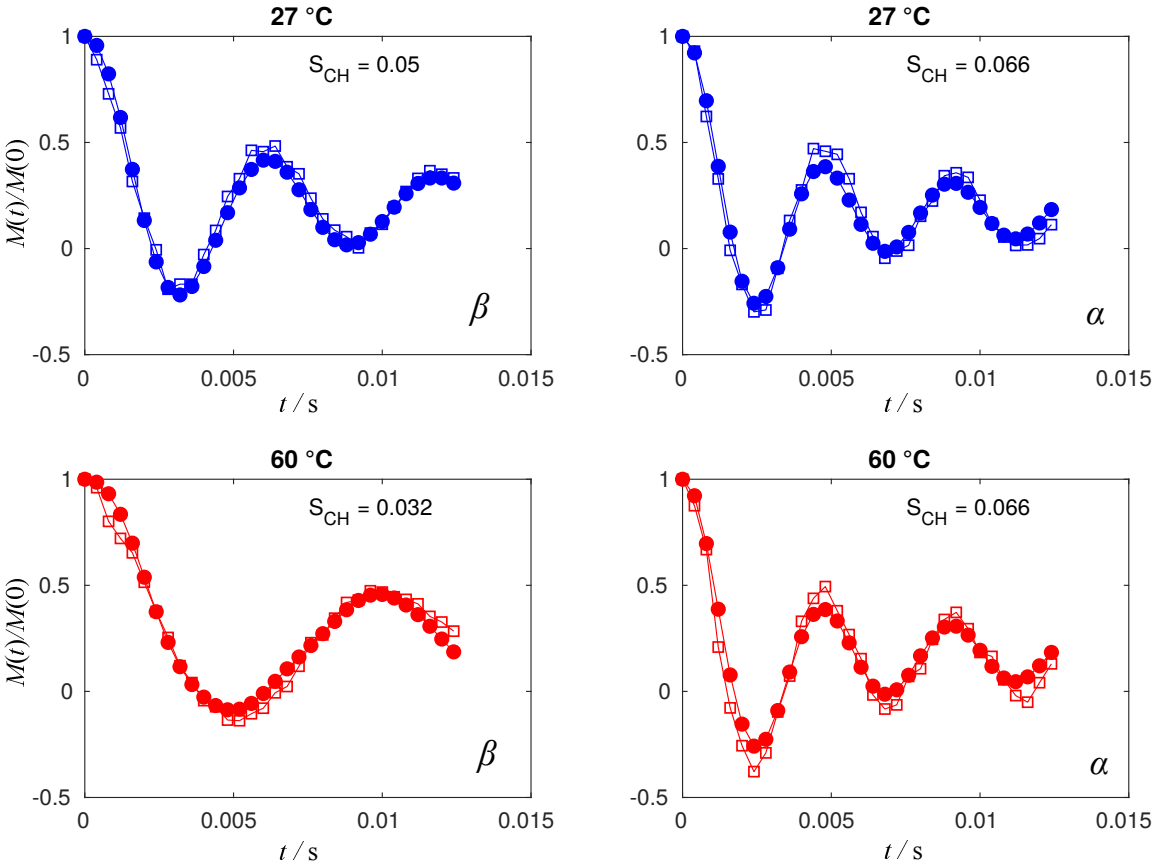

FIG. 3: R-PDLF time domain profiles from a sample of DMPC at low hydration at two different temperatures fitted with R-PDLF numerical simulations taking into account the B_1 inhomogeneity of the CP MAS probe used. The uncertainty of $|S_{\mathrm{CH}}|$ is below ± 0.005.

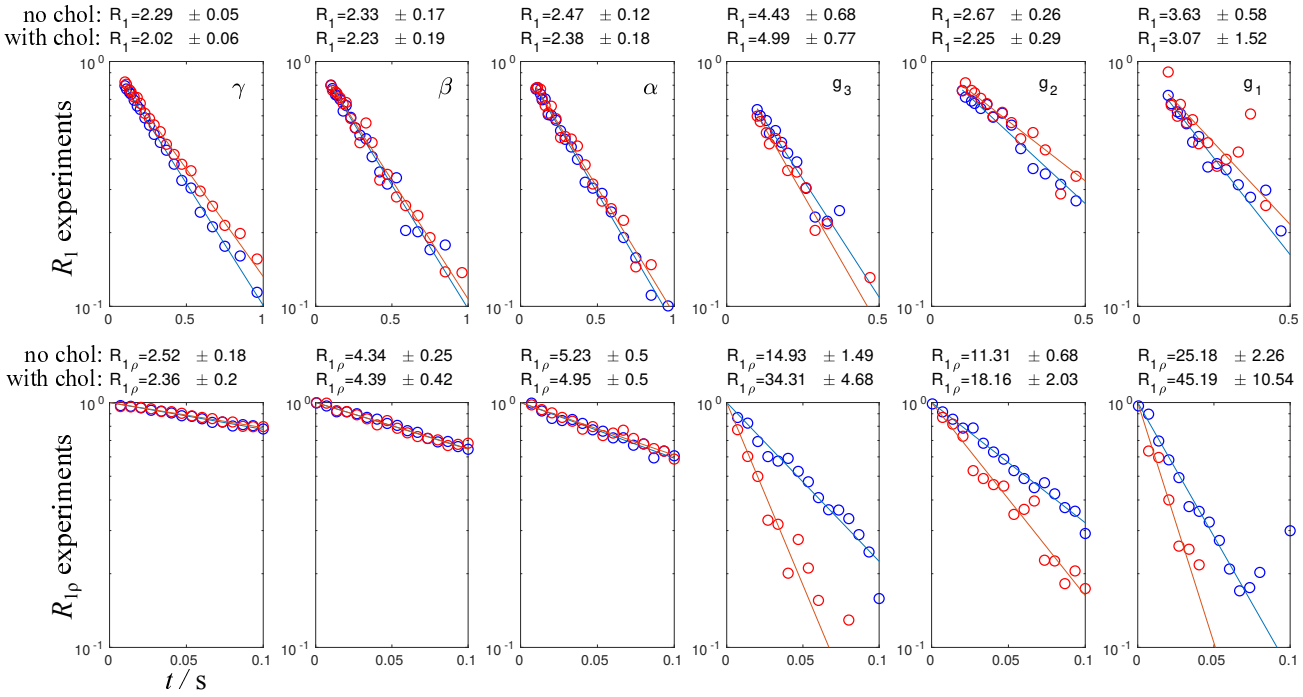

FIG. 4: The R_1 and $R_{1\rho}$ decays measured for POPC (blue) and POPC/cholesterol (red) systems. Each point corresponds to the integral determined from a gaussian fit of the corresponding ^{13}C peak in the high resolution chemical shift spectrum acquired under MAS of 5 kHz. The spin lock field for the $R_{1\rho}$ measurement was 50 kHz and the ^{13}C Larmor frequency was 125 MHz.